

Evaluation of the ultimate performances of a Ca^+ single-ion frequency standard

C. Champenois,* M. Houssin, C. Lisowski, M. Knoop, G. Hagel, M. Vedel, and F. Vedel

Physique des Interactions Ioniques et Moléculaires

Unité Mixte de Recherche 6633 CNRS-Université de Provence

Centre de Saint-Jérôme, Case C21, 13397 Marseille Cedex 20, France.

(Dated: February 20, 2019)

We numerically evaluate the expected performances of an optical frequency standard at 729 nm based on a single calcium ion. The frequency stability is studied through the Allan deviation and its dependance on the excitation scheme (single or two-Ramsey pulses). The minimum Allan deviation that can be expected is estimated to $\sigma_y(\tau) \approx 3.4 \times 10^{-15} / \sqrt{\tau}$. The frequency shifts induced by the environmental conditions are evaluated to minimize the uncertainty of the proposed standard by choosing the most suited environment for the ion. The expected relative shift is -2×10^{-16} with an uncertainty of $\pm 3 \times 10^{-16}$, if using the odd isotope $^{43}\text{Ca}^+$.

PACS numbers: 32.60.+i, 32.70.Jz, 32.80.Pj, 32.80.Qk

I. INTRODUCTION

Narrow optical transitions are considered as basis for frequency standards, thanks to the recent progress made in atom and ion cooling and trapping, laser stabilization and high-resolution optical spectroscopy. Two kinds of experiments are under study in various groups: one uses an ensemble of laser-cooled neutral atoms in a fountain, an optical lattice or a BEC, the other one uses a single trapped laser-cooled ion (for a recent review see [1]). The present work is motivated by strong progress in storing, observing, cooling and coherently manipulating single ions in Paul traps. Together with the ultra-precise optical frequency measurements achieved by frequency chains and frequency combs, these progress lead towards the realization of single-ion frequency standards, as for Hg^+ [2], Sr^+ [3, 4], Yb^+ [4] and In^+ [5], and proposed for Ca^+ [6]. Our own experimental project aims to build an optical frequency standard using the electric quadrupole transition $4S_{1/2} \rightarrow 3D_{5/2}$ of a single calcium ion at 729 nm. Among the frequency standard candidates, Ca^+ possesses the major advantage that the required radiations for cooling and exciting the clock transition can be produced by solid state lasers or diode lasers.

The performances of a frequency standard are defined by the stability of its local oscillator (a laser in the optical case) and the precision achieved in the observation of an atomic transition. Frequency instability is due to deviations from a mean frequency throughout varying probe time intervals, while frequency uncertainty is caused by the frequency fluctuations caused by environmental conditions and by the experimental conditions for observation. The quality factor of optical atomic transitions can reach 10^{15} , which is 5 orders of magnitude higher than for microwave frequency standards and thus better performances than these last standards are hoped.

In the first part of this paper we discuss the choice of the interrogation schemes which may influence on the frequency stability of a proposed frequency standard via the variation of the duration of the probe cycle. Using numerical simulations we compare single-pulse spectroscopy with time-domain Ramsey interferometry. In the second part, systematic effects expected for a standard based on $^{43}\text{Ca}^+$ that may reduce its accuracy and precision are discussed. In this paper we employ the specific parameters of the Ca^+ -ion trap experiment in Marseille [6] as an example, but we keep the manuscript as general as possible to remain applicable to other atomic species.

*caroline.champenois@up.univ-mrs.fr

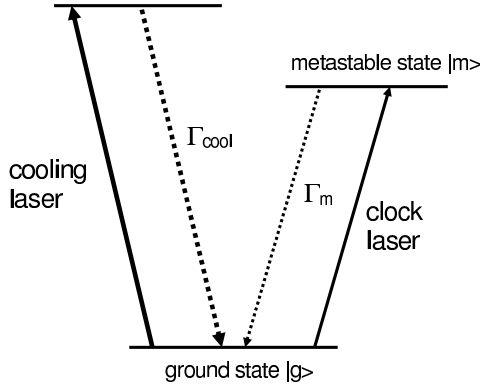


FIG. 1: Transitions involved in the cooling and probing of an ion for a frequency standard. In practice, the cooling scheme may involve several lasers because of a possible hyperfine structure and/or a possible decay towards other metastable states. The light scattered on the cooling transition is also used for detection of the ion. In most cases, Γ_{cool} is of the order of 20 MHz whereas Γ_m is of the order of 1 Hz.

II. FREQUENCY STABILITY

Frequency stability is one of the major characteristics of a frequency standard. It can be quantified by the Allan deviation $\sigma_y(\tau)$ measured for an average time τ :

$$\sigma_y(\tau) = \frac{1}{QS/N} \sqrt{\frac{T_c}{\tau}} \quad (1)$$

where $Q = f_0/\Delta f$ is the quality factor defined by the ratio of the clock frequency over its observed linewidth, S/N the signal to noise ratio and T_c the cycle time required for the interrogation of the ion.

The probe schemes for an optical transition in a single ion consist of a preparation stage, an excitation of the clock transition, and a final detection stage. The cycle time T_c is the sum of the corresponding time durations T_{prep} , T_{exc} , and T_{det} . The preparation stage implies laser cooling of the ion and optical pumping into the internal state chosen to be the ground state (see figure 1). The probing of the clock transition by the local oscillator (a laser) is done by direct laser excitation. During this stage, all the preparation lasers are shut off. After excitation of the clock transition, the cooling lasers are switched on again. The quantum jump method proposed by Dehmelt [7] allows to detect if the atom is excited or not: the absence of fluorescence signal during the detection stage proves that the ion is "shelved" in the metastable upper state whereas the presence of fluorescence signal means that the ion is still in the cooling cycle. Repetition of this measurement as a function of the clock laser frequency allows to measure the transition probability distribution. In the following, we discuss the conditions for realization and the maximum duration required for these various stages. The choice of the suited interrogation scheme minimizes the Allan deviation.

A. Preparation and detection

In this paragraph, we describe the cooling process to evaluate its duration. We suppose the ion located at the center of the trap, where the RF-trapping field is minimum and has little influence on the ion motion. Since the trap creates a harmonic potential, the motion of the ion is a superposition of oscillations at different frequencies due to the spatial anisotropy of the trapping device. If we suppose, for simplicity's sake, that there is only one frequency of motion $\omega_{tr}/2\pi$ in the trap, the resulting atomic emission spectrum is composed of a central frequency corresponding to the atomic transition $\omega_0/2\pi$ and sidebands separated by multiples of the motional frequency $(\omega_0 \pm p\omega_{tr})/2\pi$, (p integer). The sidebands are resolved if the width of each band is smaller than their mutual separation (the strong confinement condition [8]). This can be potentially achieved in miniature traps with high motional frequencies (≈ 1 MHz) for all the narrow transitions considered as potential basis for frequency standards ($\Gamma_m \ll \omega_{tr}$, see figure 1). The intensity of each band p in the spectrum depends on the oscillation amplitude X of the ion in the trap like $J_p^2(kX)$ [8] where k is the laser wavevector of the probed transition and J_p the Bessel function of order p . The functions $J_p^2(kX)$ have

negligible values when $p \gtrsim kX$ and the smaller is kX , the less sidebands are visible. Laser-cooling the ion reduces its oscillation amplitude X and thus the number of observable sidebands. A major step in the preparation of the ion is to access the Lamb-Dicke regime which is characterized by the reduction of the spectrum to one or two sidebands with a preponderant weight on the central frequency, this regime is reached if $kX \lesssim 1$.

The motion of the ion can be described by a phonon distribution, characterised by the mean phonon number $\langle n \rangle$. This vibrational state can also be characterized from the classical point of view by an oscillation amplitude $X = \sqrt{2\langle n \rangle + 1}\lambda_{tr}$, where the length $\lambda_{tr} = \sqrt{\hbar/2m\omega_{tr}}$ measures the size of the fundamental harmonic oscillator eigenstate $n = 0$. This length depends on the atom mass by $1/\sqrt{m}$ and, as an example, is equal to 11 nm for a calcium ion with $\omega_{tr} = 2\pi \times 1$ MHz. The Lamb-Dicke condition $kX \lesssim 1$ can also be expressed by $k\lambda_{tr}\sqrt{2\langle n \rangle + 1} \lesssim 1$. The Lamb-Dicke parameter $\eta = k\lambda_{tr}$ quantifies the ability for a system {ion+trap} to meet the Lamb-Dicke regime for a given transition. It is of the order of 0.1 for optical transitions (e.g. 0.095 for calcium's clock transition in the trap taken as example). In most cases, the frequency of motion in the trap is of the order of 1 MHz, whereas the atomic dipole transition used for laser cooling has a width Γ_{cool} close to $2\pi \times 20$ MHz. On such broad transition ($\Gamma_{cool}/2 \gg \omega_{tr}$) the Doppler limit for laser cooling can be approximated by the one of a free atom [8]. It leads to a thermal population of the harmonic trap levels characterized by $\langle n \rangle \simeq \Gamma_{cool}/2\omega_{tr} \simeq 10$. The Lamb-Dicke condition $\eta\sqrt{2\langle n \rangle + 1} \lesssim 1$ is then fulfilled by the phonon distribution reached by Doppler cooling ($\langle n \rangle \simeq 10$) which set the transition free of first order Doppler effect, while the second order Doppler effect is small (see section III D). Furthermore the residual phonon distribution still allows to drive coherent dynamics on the clock transition, as required for the interrogation schemes and as confirmed numerically in the following. The time needed to reach the Doppler cooling limit is of the order of milliseconds while the optical pumping is faster than the millisecond, we can thus estimate T_{prep} to 5 ms.

The duration required for the detection stage depends on the fluorescence signal collected on the strong dipole transition. For such transitions with a width of ≈ 20 MHz, one can expect at least 10^4 counts per second (cps) over a stray light level of less than 100 cps. In these conditions, 10 ms-periods are sufficient to acquire enough signal to decide if the atom has been excited or not into the metastable state. As a consequence, 15 ms is a realistic estimation for the preparation and detection contributions to the cycle duration. To this minimum cycle duration must be added the excitation duration time T_{exc} . In the following we theoretically study the minimization of this probe time for different excitation schemes.

B. Choice of the excitation scheme

The width Δf of the observed transition and its signal to noise ratio depends on the laser excitation scheme. Nevertheless, the choice of a high-frequency clock transition (in the optical domain) allows to reach smaller Allan deviations than the ones obtained on actual frequency standards in the microwave domain. Until now, the narrowest optical ion linewidth has been observed on Hg^+ [9] and has allowed to reach a relative frequency stability of 7×10^{-15} over a 1 s averaging. Here we discuss possible excitation schemes irrespective of the ion implied and we use a reduced Allan deviation $\sigma' = \sigma_y(\tau) \times f_0\sqrt{\tau}$ to quantify the expected frequency stability of the standard, keeping in mind that reduced Allan deviations between 1 and 10 have already been measured on lasers locked on an atomic optical transition.

Let p_m be the probability for the ion to be in the metastable state after excitation by the clock laser. The experimental signal used to lock a laser on the optical transition is the difference of the probability p_m measured several times on the low and high frequency sides of the transition. The equality of the two probabilities implies that the mean frequency is the center of the line. Several sources of noise can limit the signal to noise ratio. Among these is the quantum projection noise [10] which is dominant once the technical noise has been reduced. The laser excitation creates a linear superposition of the ground ($|g\rangle$) and metastable ($|m\rangle$) states $\sqrt{1-p_m}|g\rangle + \sqrt{p_m}|m\rangle$. During the detection stage, the atomic state is projected on one of these two states. The variance of such a measurement is $p_m(1-p_m)$ and implies on the measurement of the transition probability a minimal noise $\sqrt{p_m(1-p_m)}$ that can be overcome only by using squeezed states [11], which we do not consider here.

The minimum signal to noise ratio which can then be observed is

$$S/N = \sqrt{\frac{p_m}{1-p_m}}. \quad (2)$$

It is maximum for a maximum probability ($p_m = 1$). As the transition is excited on both sides of the transition line, the

measured probability p_m cannot be maximum. Furthermore, the steepest slope and so the highest frequency sensitivity is in most cases observed for p_m at half maximum on the line profile. Thus, maximum frequency sensitivity and maximum signal to noise ratio are not compatible. Additionally, the upper state finite lifetime leads to spontaneous decay which can reduce the maximum excitation probability for long excitation time.

Two excitation schemes have been experimentally tested by several groups: a single Rabi pulse and two temporally separated Ramsey pulses. The first one has been performed on Hg^+ [2], In^+ [12], Sr^+ and Yb^+ [4], and the second one on Hg^+ [2] and Sr^+ [3]. In the following we enlighten the principal features of each methods and then compare them. To quantify the relative stability allowed by the discussed methods, we evaluate the reduced Allan deviation by

$$\sigma' = \sigma_y(\tau) \times f_0 \sqrt{\tau} = \Delta f \sqrt{\frac{1-p_m}{p_m}} \sqrt{T_c} \quad (3)$$

To this purpose, numerical simulations compute the evolution of the density matrix of the two levels $|g\rangle$ and $|m\rangle$. The atomic system is defined by the metastable lifetime τ_m fixed to 1 second, and is driven by a Rabi pulsation Ω . The motion of the ion is taken into account by the phonon distribution, characterised by the mean phonon number $\langle n \rangle$. If Ω is the Rabi pulsation for the $|n=0\rangle \rightarrow |n=0\rangle$ transition, $\Omega \times L_n(\eta^2)$ is the one for the $|n\rangle \rightarrow |n\rangle$ transition, L_n being the Laguerre polynomial [13]. We choose for η , the value of 0.095 calculated for a calcium ion in the trap described as before. The linewidth Γ_L of the laser spectrum is taken into account by adding a source of decoherence equal to this width in the operator controlling the evolution of the density matrix [14]. To have maximum frequency sensitivity, the simulations compute the probability of excitation on resonance and look for the detuning needed to have half of this probability. p_m is this probability at half maximum and Δf is the full width at half maximum. For a laser detuning Δ_L and in the rotating wave approximation the matrix density evolves according to

$$\dot{\rho}_{gg} = -\dot{\rho}_{mm} = i\Omega/2 (\rho_{gm} - \rho_{mg}) + \rho_m/\tau_m \quad (4)$$

$$\dot{\rho}_{gm} = -i\Delta_L \rho_{gm} + i\Omega/2 (\rho_{gg} - \rho_{mm}) - \rho_m/2\tau_m - \Gamma_L \rho_{gm} \quad (5)$$

1. Single pulse excitation

To avoid power broadening, the narrow transition can be experimentally observed if the Rabi pulsation Ω is smaller than the linewidth and the interrogation time longer than the lifetime. But because of the finite lifetime of the excited state, the maximum excitation probability is low and requires several seconds to be reached, reducing the relative stability even if the linewidth is close to the natural width. In an ideal context where the experiment is not limited by the laser stability, the calculations show that the smallest reduced Allan variance is reached with a single pulse which should last at least 1 s and drive the transition with Ω of the order of $2 \times \Gamma_m$. With today's laser stability a cycling time of few secondes for a single measure seems not realistic. We rather consider excitation schemes with durations inferior to 1 second, since a cycle has to be repeated several times before a signal can be built up to counteract on the frequency of the local oscillator.

In figure 2, are plotted the excitation probability at half maximum p_m , the full width at half maximum Δf and the reduced stability as defined by equation (3), versus the cycle time $T_c = T_{exc} + 15$ ms, assuming a single Rabi pulse. These curves reflect Rabi oscillations, which show maximum excitation probability for $T_{exc} = (2p+1)\pi/\Omega$. The interesting feature is the minimum of the reduced Allan variance observable for the shortest T_{exc} . Two cases with different Rabi pulsation Ω ($\Omega = 10 \times \Gamma_m$ and $\Omega = 100 \times \Gamma_m$) are compared in figure 2. For both cases, excitation probability and full width at half maximum are computed for an ion whose oscillatory motion (or phonon distribution) is corresponding to the Doppler cooling limit ($\langle n \rangle = 10$) or to cooling to the fundamental vibrational state ($\langle n \rangle = 0$). The first result to mention is that the first minima of the reduced Allan variance are identical for these two phonon distributions, for the chosen Rabi pulsation, thus confirming that Doppler cooling is sufficient for state preparation. The results shown on figure 2 suggest that the discrepancy between the $\langle n \rangle = 10$ and the $\langle n \rangle = 0$ phonon distribution increases with the pulse duration. We have checked that in the case of the short pulses we consider in the following, the results are nearly the same for these two thermal phonon distributions and thus, from now on, only the cases concerning $\langle n \rangle = 0$ are dealt with.

To illustrate on figure 2 the influence of the strength of the Rabi pulsation, the excitation is driven by $\Omega = 10 \times \Gamma_m$ and $\Omega = 100 \times \Gamma_m$. In the first case, the minimum reduced Allan deviation is close to 1 but requires to excite for

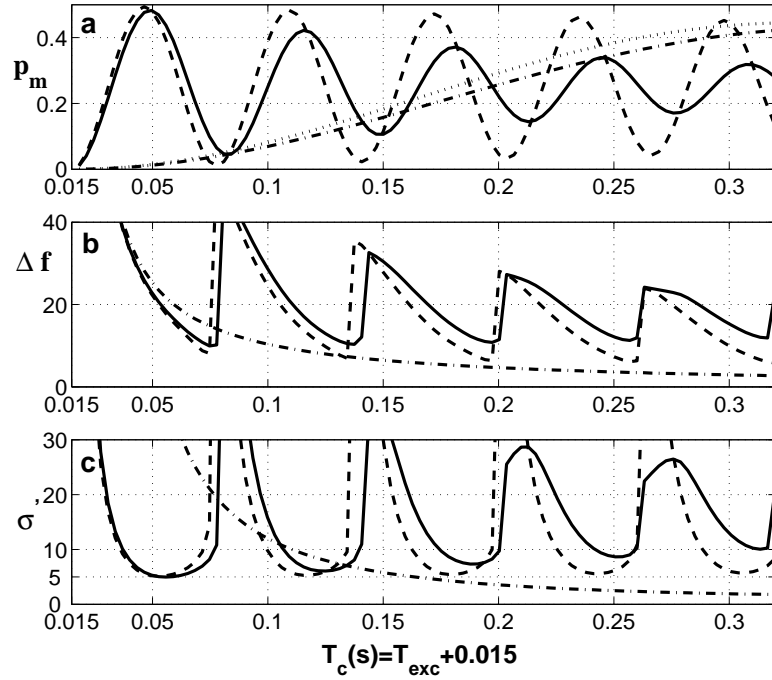


FIG. 2: calculations for a metastable lifetime $\tau_m = 1$ s and a single Rabi pulse, for two thermal phonon distributions. (a): probability p_m to be in the metastable state at half maximum, (b): full width at half maximum Δf (Hz), (c): reduced relative stability σ' , versus the cycle duration T_c .

dotted line: $\Omega = 10 \times \Gamma_m$ and $\langle n \rangle = 0$, dash-dotted line: $\Omega = 10 \times \Gamma_m$ and $\langle n \rangle = 10$, broken line: $\Omega = 100 \times \Gamma_m$ and $\langle n \rangle = 0$, solid line: $\Omega = 100 \times \Gamma_m$ and $\langle n \rangle = 10$.

On (b) and (c), the dotted and dash-dotted line ($\Omega = 10 \times \Gamma_m$ and $\langle n \rangle = 0$ or 10) are almost superposed and only one curve is plotted on the graph.

more than 300 ms. In the second case, the first minima is reached for a cycle duration of 50 ms, but this shortening of the cycle duration is paid by an increase of σ' equal to 4.5. This trend is general and a further increase of the Rabi pulsation leads to an increase of the minimum Allan deviation as well as a decrease of the required cycle time.

We now take into account the effect of a finite laser linewidth on the minimum reduced Allan deviation and compare the value computed for a laser narrower than the atomic transition ($\Gamma_L/2\pi = 0.1$ Hz) to the one computed with an achievable 10 Hz broad laser. In this later case, the performance of the clock are greatly reduced first by the reduction of the excitation probability and second by the broadening of the observed transition. The first drawback can be overcome by the increase of the Rabi pulsation but this is paid by a further increase of the transition broadening. As a consequence, for a given laser linewidth and a given metastable lifetime, there is an optimal Rabi pulsation which results in a minimal reduced Allan deviation. This is illustrated on figure 3 where for $\Gamma_L/2\pi = 10$ Hz, σ' is minimal for $100 \times \Gamma_m \lesssim \Omega \lesssim 125 \times \Gamma_m$ and is then equal to 12.4 for a cycle time of 40 ms, whereas for $\Gamma_L/2\pi = 0.1$ Hz, σ' is minimal for $\Omega \simeq 4\Gamma_m$ and is then equal to 1.7 but for a cycle time of 625 ms.

2. Comparison with Ramsey interferometry

The introduction of the separated fields method or Ramsey interferometry [15] was soon followed by breakthroughs in high resolution spectroscopy and is expected to overcome the limitations met with single pulse excitation. With this method the line profile is recorded after two pulses of duration T such as $\Omega T = \pi/2$, separated by a free evolution time T_{free} . When the laser detuning is scanned, the profile show Ramsey fringes resulting from an interference pattern and for short enough pulse duration, the width of the central fringe is equal to $1/2T_{free}$ and is then independent from the Rabi pulsation. For a chosen pulsation Ω , the evolution of p_m , Δf and σ' does not show oscillations with T_c , like for a single Rabi pulse. σ' takes very high values for short T_c and decreases toward a limit for longer T_c . This limit depends on the choice of the pulsation Ω . To compare the Rabi and Ramsey excitation scheme, we looked for the

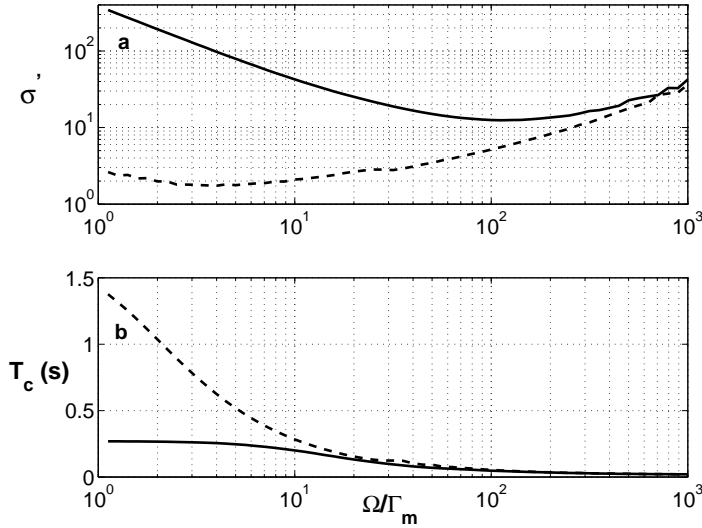


FIG. 3: (a): Minimum reduced Allan deviation and (b): cycle duration T_c required to reach this minimum versus the Rabi pulsation. Computation done for a metastable lifetime $\tau_m = 1$ s and a single Rabi pulse by a laser of width Γ_L , with a thermal phonon distribution characterised by $\langle n \rangle = 0$. broken line: $\Gamma_L/2\pi = 0.1$ Hz and solid line: $\Gamma_L/2\pi = 10$ Hz.

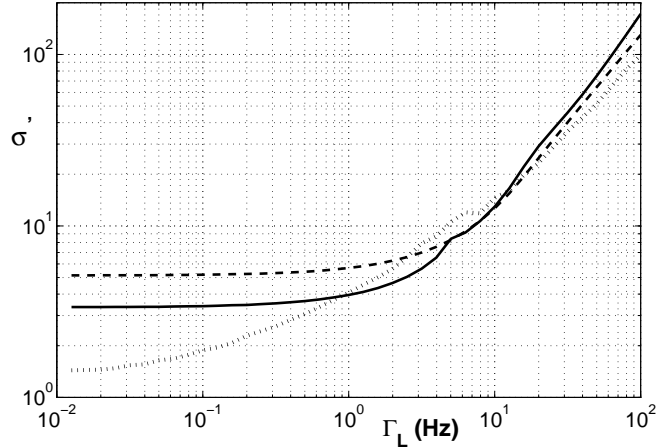


FIG. 4: Minimum reduced Allan deviation versus the laser linewidth Γ_L (Hz), for a metastable lifetime $\tau_m = 1$ s. The dotted line shows the minimal achievable reduced deviation when the cycle time and the pulsation are unlimited (Rabi or Ramsey method). The dashed (solid) line shows the minimal deviation achievable with a cycle time fixed to 50 ms, with a single rabi pulse (two Ramsey pulses) excitation.

minimal reduced Allan deviation reached with both method for a given laser linewidth and for different cycle time. This study shows that there is little differences between the performances allowed by these two methods. Nevertheless, the Ramsey method is more advantageous with laser narrower than 5 Hz whereas for broader laser, the Rabi method gives slightly better results. These features are summarized on figure 4 where the minimum reduced Allan deviation is plotted for a laser linewidth from 0.01 to 100 Hz. Two different cases are then studied. On one hand, the minimal deviation is searched with no limitations on T_c nor Ω . Then, the Ramsey or Rabi method gives nearly the same results and only one of them is plotted on figure 4. The minimal achievable reduced deviation is 1.4 for Rabi and 1.3 for Ramsey method, for an ultra-narrow laser. The Ramsey method requires 3.5 s to reach its limit, which is more than three times longer than the time required by a single Rabi pulse.

On the other hand, the minimal deviation is searched for a cycle time fixed to 50 ms. For a single Rabi pulse, it implies a pulsation $\Omega \simeq 95 \times \Gamma_m$ as long as Γ_L is smaller than 10 Hz. For broader laser, the required pulsation increases to $160 \times \Gamma_m$ for $\Gamma_L = 100$ Hz. The behaviour is different for a two Ramsey pulses excitation. A given cycle

time does not decide for an optimal value but a minimal value for the pulsation. In practice, for laser linewidths smaller than 5 Hz, the reduced Allan deviation reaches its limit with 0.3 % accuracy if $\Omega = 10^3 \times \Gamma_m$ and with 0.03 % accuracy if $\Omega = 10^4 \times \Gamma_m$. To reduce the light-shift induced by the clock laser (see section III C), we set $\Omega = 10^3 \times \Gamma_m$. For $\Gamma_L > 5$ Hz, better results are reached for a lower pulsation of $\Omega = 100 \times \Gamma_m$. In these conditions, a Ramsey excitation allows to reach a reduced deviation of 3.3 and a Rabi excitation a deviation of 5.1, for a laser as narrow as the atomic transition. The reduced deviation remains smaller than 10 as long as $\Gamma_L \leq 5$ Hz.

As a conclusion, if the cycle time is not limited by the oscillator stability, an optical atomic clock can reach reduced Allan deviation of 1.4, with a single Rabi pulse as well as with two separated Ramsey pulses. As an example, with the clock transition at 282 nm in Hg^+ , this could result in an Allan deviation of $\approx 1.4 \times 10^{-15}/\sqrt{\tau}$ whereas with the clock transition at 729 nm in Ca^+ , it could result in $\sigma_y(\tau) \approx 3.4 \times 10^{-15}/\sqrt{\tau}$. If, for technical reasons, the cycle time has to be shortened to the 100 ms range, a Ramsey scheme is more appropriate to take advantage of a very narrow transition, if the laser linewidth is smaller than 5 Hz.

III. FREQUENCY STANDARD ACCURACY AND PRECISION

The second relevant set of parameters defining a frequency standard are its accuracy and precision. The standard frequency may be shifted from the atomic value by any interaction of the atom with external fields. If this shift is constant, it only reduces the standard accuracy but not its precision. If this shift varies in time or can not be evaluated precisely, the precision is reduced also. Since all this contributes to the uncertainty of the future frequency standard, all the interactions of the ion with its surrounding must be controlled to minimise and/or make constant any shift of the standard frequency. Here we evaluate these shifts for a calcium ion in order to choose the best internal state and environment for which they are minimum.

The ground state $|g\rangle$ of the calcium ion is $S_{1/2}$ and the metastable state $|m\rangle$ is $D_{5/2}$ with a measured lifetime of 1152 ± 23 ms [16] which leads to a natural width for the clock transition of 138 ± 3 mHz. We require that during the excitation of the transition by the clock laser, all other lasers are shut off. This makes sure that there are no light-shifts of the levels $S_{1/2}$ and $D_{5/2}$ caused by the cooling lasers. The other major effects that can shift the standard frequency are due to the local magnetic and electric fields and to the power of the clock laser itself. In the Lamb-Dicke regime, only the second order Doppler effect shifts and broadens the line. We first focus on the Zeeman effect as it governs the choice of the isotope and atomic sublevels used for the standard.

A. Zeeman effect

To avoid any uncontrolled or non-stable shifts, the frequency standard must be made as independent as possible of environmental conditions. The first order Zeeman effect can be straightly eliminated by the use of atomic Zeeman sublevels with no projection of the total moment on the magnetic field ($m = 0$). The solution is to use an isotope with a half integer nuclear spin. The most abundant one (0.135%) is $^{43}\text{Ca}^+$ with a nuclear spin $7/2$. The hyperfine structure of this isotope can be found on figure 5. The second order Zeeman shift depends on the choice of the hyperfine sublevels. We calculate these shifts by searching the eigenvalues of the Zeeman Hamiltonian for the $|F, m_F\rangle$ states. The Zeeman shift of the fundamental hyperfine levels $|S_{1/2}, F = 3 \text{ or } 4, m_F = 0\rangle$ are at least 2 orders of magnitude smaller than the shift of the metastable hyperfine levels $|D_{5/2}, F = 1, \dots, 6, m_F = 0\rangle$ and are not relevant for the choice of the level to use. Figure 6 shows the quadratic Zeeman shifts for the different hyperfine levels of $D_{5/2}$ for sublevels $m_F = 0$. These curves illustrate the great variation of these shifts with the hyperfine sublevel. Depending on the level involved, the second order Zeeman effect can be as large as $98.04 \text{ Hz}/\mu\text{T}^2$ for $F = 1$ or reduced to $-9.05 \text{ Hz}/\mu\text{T}^2$ for $F = 6$ (see figure 6). This last level should be used as basis for the standard to reduce the second order Zeeman effect. As the $S_{1/2} \rightarrow D_{5/2}$ transition is electric-quadrupole, the selection rules $\Delta F = 0, \pm 1, \pm 2$ imply that the fundamental sublevel involved in the standard should be $|S_{1/2}, F = 4, m_F = 0\rangle$.

To eliminate the uncertainty due to the Zeeman effect, the local magnetic field must be kept on the $0.1 \mu\text{T}$ level. Still, a controlled magnetic field is needed to split all the Zeeman sublevels and be able to select the $m_F = 0 \rightarrow m_F = 0$ transition. The two closest transitions $|S_{1/2}, 4, \pm 1\rangle \rightarrow |D_{5/2}, 6, \pm 1\rangle$ are split apart by $\pm 3.5 \text{ kHz}/\mu\text{T}$. So a magnetic field of $0.1 \mu\text{T}$ allows to isolate the $m_F = 0 \rightarrow m_F = 0$ transition and can be measured by the observation of these neighbouring transitions. Nevertheless, such a magnetic field may not be sufficient to maintain a high level

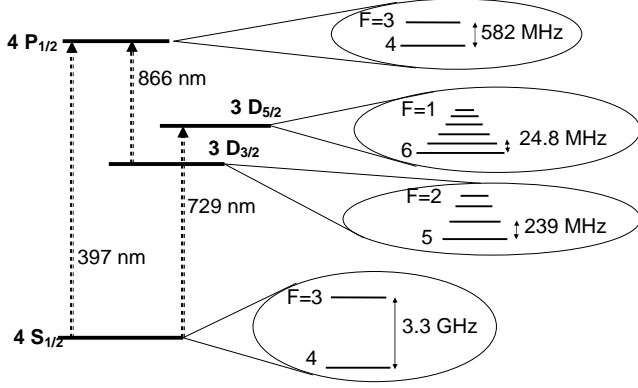


FIG. 5: Hyperfine structure of the levels involved in the preparation, excitation and detection of $^{43}\text{Ca}^+$ [17, 18].

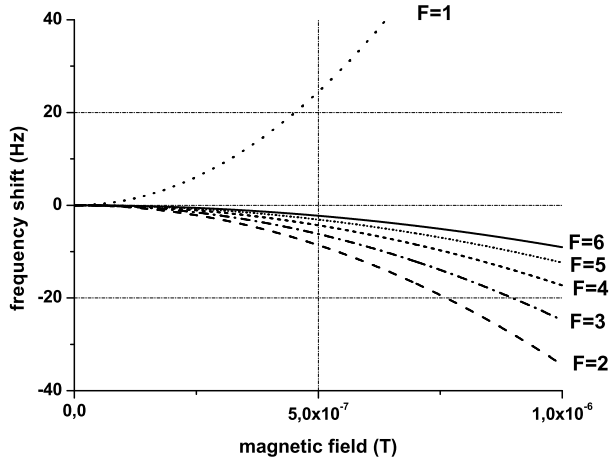


FIG. 6: Zeeman shift of the metastable hyperfine sublevels of $D_{5/2}$ versus the magnetic field, for Zeeman sublevel $m_F = 0$.

of scattered light by the atomic system, as observed for other ions under study [4]. But it is possible to recover a high level signal by spinning of the laser polarisation [4, 19] and we do not consider this reduction of the signal as a limitation. Without any magnetic field applied, the local field caused by the earth and the close surrounding is of the order of 0.01 T whereas such fields can be produced by 1 A in Helmholtz coils. Furthermore, magnetic field fluctuations of $0.2 \mu\text{T}$ over one day have been observed in an unshielded environnement [20]. As a consequence, in a thermalized and shielded environnement, it is technically possible to compensate for the already existing magnetic field and to add the desired magnetic field of $0.1 \pm 0.05 \mu\text{T}$ with available current supplies of 1 A stabilized to the mA level. In these conditions, the frequency uncertainty due to the Zeeman effect is

$$B = 0.1 \pm 0.05 \mu\text{T} \rightarrow \delta f_Z = -0.09 \pm 0.09 \text{ Hz} \quad (6)$$

It is possible to prepare the atomic system in the $|S_{1/2}, F = 4, m_F = 0\rangle$ state thanks to the property of dipole transition that forbids $|F, m_F = 0\rangle \rightarrow |F, m_F = 0\rangle$ transitions. After the cooling stage, two lasers polarised parallelly to the magnetic field ($\Delta m_F = 0$) and resonant with the $|S_{1/2}, F = 4$ and $F = 3\rangle \rightarrow |P_{1/2}, F = 4\rangle$ transitions optically pump the system in the $|S_{1/2}, F = 4, m_F = 0\rangle$ state in few microseconds, then ready for the probe stage. Actually, the cooling and optical pumping stage are not so simple due to a possible decay from $P_{1/2}$ to $D_{3/2}$ level (see figure 5), whose lifetime is the same order of magnitude as $D_{5/2}$ and so requires three repumping lasers, to empty the possibly occupied $F = 3, 4, 5$ levels. If the repumping lasers are $\sigma = \sigma^+ + \sigma^-$ polarised, the cooling and optical pumping

remains efficient, as long as the three repumping lasers' detuning is different from the two cooling ones, to avoid black resonances [21] and as long as the polarization is spun to prevent pumping into dark states [19].

B. Shifts due to interaction with DC electric fields

The second order Stark effect shifts the standard frequency through the coupling of the levels $S_{1/2}$ and $D_{5/2}$ to all the other atomic levels by electric dipole interaction with any DC or slowly varying electric fields. These fields also shift the $D_{5/2}$ level by the coupling of its electric quadrupole moment to any electric field gradient. In a usual miniature spherical trap, the confining electric field has no static component, oscillates at a frequency of the order of 10 MHz and its shape in its center can be very well approximated by a quadrupole. In the exact center of the trap there should be no oscillating field but an oscillating field gradient. However, in a real Paul trap, patch potentials deform the harmonic potential well created by the RF field. They separate the minimum potential point from the zero RF-field point and static bias voltages have to be applied in the three directions to make these two points meet again and reduce any static field smaller than V/cm. This step is required to be able to cool an ion to the Doppler limit and reach the Lamb-Dicke regime [22] and can lead to an increase of the static electric field gradient. Such gradient can realistically reach 1V/mm on 1 mm (the typical diameter of a Paul-Straubel trap). The local electric field is then the sum of the quadrupole oscillating field that traps the ion, the bias static field lower than V/cm and the isotropic field radiated by the vessel considered as a blackbody. Since the frequencies of this radiated field are far under the optical resonance of Ca^+ , the field can be taken into account by its mean-square value averaged over all the blackbody spectrum, whose value is given by [23]

$$\langle E_{BB}^2 \rangle = 831.9^2 \left(\frac{T}{300} \right)^4 \quad (7)$$

in (V/m)² with T in Kelvin. At room temperature, this field overtakes the static bias field resulting from compensation of patch potentials. Nevertheless, it can be drastically reduced by cooling of the vessel and a thermalization at 77 K sets this field under the level of V/cm, to be compared to the bias static one.

Thanks to a symmetry property of the second order Stark Hamiltonian (which behaves like a second order tensor), the Stark shift of $S_{1/2}$ is independent of the hyperfine level and Zeeman sublevel. As a consequence, it is also independent of the polarisation of the electric field and behaves like a scalar (this property is true for any level with $J < 1$). An electric field couples the ground state $4S_{1/2}$ to all the $nP_{1/2}$ and $nP_{3/2}$ levels but in the fact, the sum of the oscillator strength on $4P_{1/2}$ and $4P_{3/2}$ is already equal to 1 [24] and there is no point taking into account other couplings to $n > 4$ levels. The second order Stark shift on $4S_{1/2}$ is then easily evaluated to $-9.5 \text{ mHz}/(\text{V/cm})^2$.

The Stark effect on the $D_{5/2}$ level can be split into a scalar term, independent on F and m_F and a tensorial part, depending on these two quantum numbers and on the angle θ between the electric field and the magnetic field defining the quantification axis. The sum of all the oscillator strengths of the transitions between $3D_{5/2}$ and $nP_{3/2}(n \geq 4)$, $nF_{5/2}(n \geq 4)$ and $nF_{7/2}(n \geq 4)$ is only 0.48 (according to the Harvard database [24]), suggesting that there are other couplings with levels belonging to the continuum. Then our evaluation can only be a rough estimation, but it gives a correct order of magnitude. We find $-3.9 \text{ mHz}/(\text{V/cm})^2$ for the scalar part and $+2.1 \text{ mHz}/(\text{V/cm})^2 \times (3 \cos^2 \theta - 1)/2$ for the tensorial part and associate an uncertainty as high as the value itself to take into account that there are missing couplings. The total frequency shift due to DC-Stark effect is then

$$\delta f_S(S_{1/2} \rightarrow D_{5/2}, F = 6, m_F = 0) = 5.7(\pm 4) + 2.1(\pm 2) \times \left(\frac{3 \cos^2 \theta - 1}{2} \right) \text{ mHz}/(\text{V/cm})^2 \quad (8)$$

At room temperature, the DC Stark shift is mainly due to the isotropic radiated field and is

$$\delta f_S(S_{1/2} \rightarrow D_{5/2}, F = 6, m_F = 0) = 0.39(\pm 0.27) \text{ Hz.} \quad (9)$$

If the vessel is cooled to 77 K, the contribution of the radiated field is of the same order as the bias static field so its direction is unknown and its amplitude of the order of 1 V/cm. Such a field induces an uncertainty on the frequency of

$$\delta f_S(77K)(S_{1/2} \rightarrow D_{5/2}, F = 6, m_F = 0) \leq 12 \text{ mHz.} \quad (10)$$

As for the coupling of the electric quadrupole moment of $3D_{5/2}$ to any electric field gradient, it depends on the hyperfine level and its Zeeman sublevel and on the shape as well as on the symmetry axis of the electric potential [25]. The coupling strength is due to a non spherical repartition of the electronic charge density and depends on the atomic orbitals of the considered level. The quadrupole moment $\Theta(3D_{5/2})$ of the fine structure state can be defined as [25]

$$\Theta(3D_{5/2}) = -\frac{e}{2} \left\langle 3D_{5/2}, m_J = \frac{5}{2} \middle| 3z^2 - r^2 \middle| 3D_{5/2}, m_J = \frac{5}{2} \right\rangle. \quad (11)$$

This is calculated by considering the electronic orbital of $3D_{5/2}$ as pure $3d$ without any mixing with other electronic states. For a single electron atom [26]

$$\Theta = \frac{e}{2} \langle r^2 \rangle \frac{2J-1}{2J+2}. \quad (12)$$

In our case

$$\Theta(3D_{5/2}) = -\frac{2e}{7} \langle r^2 \rangle_{3d}, \quad (13)$$

the opposite sign is due to a charge distribution caused by an electron hole in a closed shell, in agreement with [25], where the Cowan code is used to compute $\langle r^2 \rangle_{5d}$ for Hg^+ . A good enough and simple estimation of $\langle r^2 \rangle$ in alkali like ion is provided by the quantum defect method [27] which gives for Ca^+

$$\langle r^2 \rangle_{3d} = 6.6a_0^2 \quad (14)$$

where a_0 is the Bohr radius. The energy shift of the hyperfine sublevel $|F = 6, m_F = 0\rangle$ of $3D_{5/2}$ is

$$\delta E = \frac{7}{11} \left(-\frac{2e}{7} \langle r^2 \rangle_{3d} \right) \left(\frac{1}{2} \frac{\partial^2 V}{\partial x^2} \right) \Pi \quad (15)$$

where Π is a geometrical factor equal to $(3 \cos^2 \beta - 1)$ if the field has a quadrupole symmetry ($V \propto x^2 + y^2 - 2z^2$), β being the angle between its symmetry axis and the magnetic field defining the quantization axis. The frequency shift of the standard transition under investigation is then

$$\delta f = -8.1 \times 10^{-7} \left(\frac{1}{2} \frac{\partial^2 V}{\partial x^2} \right) \Pi \quad \text{Hz} \quad (16)$$

The hyperfine level has little influence on this shift as, for exemple, $7/11$ is replaced by $17/35$ for the level $F = 2$. With the expected gradient of 1 V/mm over 1 mm, the uncertainty induced by this effect reaches the Hertz level, which is a lot compared to the width of the clock transition in Ca^+ . Any modification of the patch potential, due for exemple to the ion creation process, alters this shift and reduces the reproductibility of the standard. Still, this effect can be eliminated by averaging the transition frequency measured with the magnetic field along three perpendicular directions, as the geometrical Π factor is then averaged to zero [25]. The remaining uncertainty will then depend on the precision of the angle setting between the three measures. This precision will depend a lot on the vessel design and experimental setup, thus it seems difficult to estimate such an uncertainty as long as we have not performed such a measure. Nevertheless, other authors [28] have projected to reduce by 50 the uncertainty induced by this shift and we assume that a reduction by a factor of 10 is achievable, which set the uncertainty induced by this quadrupole effect to ± 0.1 Hz. At this point, it is important to mention that in spherical miniature trap, the field gradient is lower than in a linear trap, due to the confining geometry. As a consequence, a spherical trap must be preferred to a linear trap to minimize the shift induced by such gradient and thus the frequency uncertainty.

C. Shifts due to interaction with AC electric fields

During the excitation, only the clock laser is involved. It can still cause an AC-Stark shift (or light-shift) of $S_{1/2}$ and $D_{5/2}$ by coupling them to $P_{1/2}$ and $P_{3/2}$ by dipole interaction or by coupling them to other Zeeman sublevels of $D_{5/2}$ and $S_{1/2}$ by quadrupole interaction (the coupling with $D_{3/2}$ is far less strong). The first two couplings produce

a shift proportionnal to the laser intensity I_{729} equal to $1.1 \times 10^{-4} \times I_{729}$ Hz. The laser intensity required to produce the highest Rabi pulsation of 1000 s^{-1} considered in part II B 2 on the $|S_{1/2}, 4, 0\rangle \rightarrow |D_{5/2}, 6, 0\rangle$ transition is $0.75 \mu\text{W/mm}^2$, which leads to a light-shift caused by dipole coupling equal to 0.08 mHz , which is negligeable compared to the natural width of the transition.

Light-shifts of a few kHz due to quadrupole interaction with other Zeeman sublevels have been measured on $^{40}\text{Ca}^+$ isotope [29]. In these experiments Rabi pulsations of 1 MHz were used with laser detunings of the order of 1 MHz also. We calculated this shift in the context of the clock transition excitation for a Rabi pulsation equal to 1000 s^{-1} and a magnetic field of $0.1 \mu\text{T}$. The frequency detuning required to probe the clock transition depends on the laser linewidth and the Rabi pulsation used, it is of the order of 1 Hz and by choosing $\pm 10 \text{ Hz}$ for this detunings the light-shift effect is not underestimated. We find for these parameters an effect equal to $\pm 6 \text{ mHz}$ and decreasing to $\pm 0.06 \text{ mHz}$ if the magnetic field is $1 \mu\text{T}$. The sign depends on the sign of the detuning. Two reasons make this effect very small: the small Rabi pulsation considered for such experiments and the small detuning required to probe the two sides of the transition (of the order of few Hz). With such small detuning, the couplings of $|S_{1/2}, 4, 0\rangle$ with $|D_{5/2}, 6, 2\rangle$ and with $|D_{5/2}, 6, -2\rangle$ compensate each-other (and vice-versa for $|D_{5/2}, 6, 0\rangle$ with $|S_{1/2}, 4, \pm 2\rangle$). Nevertheless, with the laser power and magnetic field values planned for the optical clock realisation, this effect overtakes the ones induced by dipole couplings.

D. Second order Doppler shift

The second order Doppler effect shifts the frequency transition by

$$\frac{\delta f_D}{f_0} = -\frac{\langle v^2 \rangle}{2c^2} \quad (17)$$

With an oscillating ion, cooled to the Doppler limit, the velocity of the ion can be written like $v = V_0 \cos(\omega_{tr}t + \phi)$ and $\langle v^2 \rangle = V_0^2/2$. This mean-square velocity is calculated by $V_0 = \omega_{tr}X$ and $X = \sqrt{2\langle n \rangle + 1}\lambda_{tr}$ (cf II A). With the values chosen in II A, the velocity amplitude $V_0 = 0.32 \text{ m/s}$ leading to a second order Doppler relative shift

$$\frac{\delta f_D}{f_0} = -2.8 \times 10^{-19} \quad (18)$$

In the case of the Ca^+ clock transition ($f_0 = 4.11 \times 10^{14} \text{ Hz}$), the absolute shift is 0.11 mHz , which is negligeable in the reduction of the clock precision. This calculation confirms that Doppler laser cooling is sufficient also to reduce the second order Doppler effect to negligeable values.

E. Uncertainty budget

Table I gives the uncertainty budget expected for an atomic clock based on $^{43}\text{Ca}^+$. At room temperature, and with the considered magnetic field, the major source of frequency shift and uncertainty is the Stark effect induced by the radiated electromagnetic field. This effect is drastically reduced in a vessel cooled to 77 K and then the major source of uncertainty becomes the coupling with the field gradient through the quadrupole moment of $D_{5/2}$ which can not be reduced by cooling the vessel nor by controlling the ion position inside the trap and limits the ultimate precision of the clock. It can be compensated by measuring the frequency with three perpendicular directions of magnetic field, but the obtained precision will depend on the design of the experimental setup and the ability to control the directions of the laser propagation and magnetic field. The projections made for all these major systematic shifts show that a standard based on $|S_{1/2}, 4, 0\rangle \rightarrow |D_{5/2}, 6, 0\rangle$ of $^{43}\text{Ca}^+$ can reach an uncertainty of 3×10^{-16} , with room for improvement.

IV. CONCLUSION

We have presented a theoretical evaluation of the ultimate performances that can be expected from an optical frequency standard based on an electric quadrupole transition of a trapped single $^{43}\text{Ca}^+$ ion. We studied its stability

TABLE I: Uncertainty budget for the transition $|S_{1/2}, 4, 0\rangle \rightarrow |D_{5/2}, 6, 0\rangle$ in $^{43}\text{Ca}^+$

effect	fields/conditions	frequency shift (Hz)@ 300 K	@ 77 K
second order Zeeman effect	0.1 μT	-0.09 ± 0.09	-0.09 ± 0.09
Stark effect	radiated and bias static field	0.39 ± 0.27	≤ 0.012
$D_{5/2}$ coupled to the field gradient	1 V/mm ²	± 0.1	± 0.1
AC Stark effect	0.75 $\mu\text{W/mm}^2$ @ 729 nm, 0.1 μT	± 0.006	± 0.006
second order Doppler effect	ion cooled to the Doppler limit	1×10^{-4}	2×10^{-4}
global shift and uncertainty		$+0.3 \pm 0.3$	-0.09 ± 0.13
relative shift and uncertainty		$+7(\pm 7) \times 10^{-16}$	$-2 (\pm 3) \times 10^{-16}$

through its Allan deviation, assuming that the signal to noise ratio would be limited by the quantum projection noise. Our results show that a frequency instability of $\approx 3.4 \times 10^{-15}/\sqrt{\tau}$ can be expected. We also show that if there is no limitation on the cycle duration a single Rabi pulse can be used as well as two Ramsey pulses whereas this last scheme is to be preferred if the cycle time has to be limited to 50 ms, as long as the laser linewidth is narrower than 5 Hz. Furthermore, compared to an ultra-narrow laser, the frequency instability is increased by a factor of 10 if the laser linewidth is wider than 20 Hz.

All the systematic frequency shifts have been estimated and the environmental conditions studied in order to minimize the frequency uncertainty. This is limited by the precision reached in the successive orientation of 3 mutually perpendicular magnetic fields to compensate the coupling of the $D_{5/2}$ quadrupole with a field gradient. A technical challenge for the future optical frequency standard will be to point these three perpendicular magnetic fields and to reduce the field gradient. In this context, a miniature spherical trap is more appropriate than a linear one to a frequency standard. Our projections show that with a first step alignment, a standard based on $|S_{1/2}, 4, 0\rangle \rightarrow |D_{5/2}, 6, 0\rangle$ of $^{43}\text{Ca}^+$ can reach an uncertainty of 3×10^{-16} , an order of magnitude smaller than the most precise actual frequency standard [30].

Acknowledgement

The authors would like to thank F. Schmidt-Kaler for very helpful discussions. Our project has been supported by the Bureau National de Métrologie.

[1] E. Braun and J. Helmcke, (Eds) *Meas. Sci. Technol.* **14**, 1159 (2003).
[2] R. Rafac, B. Young, J. Beall, W. Itano, D. Wineland, and J. Bergquist, *Phys. Rev. Lett.* **85**, 2462 (2000).
[3] L. Marmet and A. Madej, *Can. J. Phys.* **78**, 495 (2000).
[4] P. Gill, G. Barwood, H. Klein, G. Huang, S. Webster, P. Blythe, K. Hosaka, S. Lea, and H. Margolis, *Meas. Sci. Technol.* **14**, 1174 (2003).
[5] M. Eichenseer, A. Y. Nevsky, C. Schwedes, J. von Zanthier, and H. Walther, *J. Phys. B* **36**, 553 (2003).
[6] C. Champenois, M. Knoop, M. Herbane, M. Houssin, T. Kaing, M. Vedel, and F. Vedel, *Eur. Phys. J. D* **15**, 105 (2001).
[7] H. Dehmelt, *Advances in Atomic and Molecular Physics* **3**, 53 (1967).
[8] D. Wineland and W. Itano, *Phys. Rev. A* **20**, 1521 (1979).
[9] S. Diddams, T. Udem, J. Bergquist, E. Curtis, R. Drullinger, L. Hollberg, W. Itano, W. Lee, C. Oates, K. Vogel, et al., *science* **293**, 825 (2001).
[10] W. Itano, J. Bergquist, J. Bollinger, J. Gilligan, D. Heinzen, F. Moore, M. Raizen, and D. Wineland, *Phys. Rev. A* **47**, 3554 (1993).
[11] D. Wineland, J. Bollinger, W. Itano, and D. Heinzen, *Phys. Rev. A* **50**, 67 (1994).
[12] T. Becker, J. v.Zanthier, A. Y. Nevsky, C. Schwedes, M. Skvortsov, H. Walther, and E. Peik, *Phys. Rev. A* **63**, 051802R (2001).
[13] C. Blockley, D. Walls, and H. Risken, *Europhys. Lett.* **17**, 509 (1992).
[14] C. Cohen-Tannoudji, *Frontiers in laser spectroscopy, Les Houches 1975* (North-Holland, 1977), p. 58.
[15] N. Ramsey, *Molecular beams* (Oxford, 1956).

- [16] M. Knoop, C. Champenois, G. Hagel, M. Houssin, C. Lisowski, M. Vedel, and F. Vedel (2003), submitted to E.P.J.D, arXiv physics/0309094.
- [17] F. Arbes, M. Benzing, T. Gudjons, F. Kurth, and G. Werth, Z. Phys. D **31**, 27 (1994).
- [18] W. Nrtershuser, K. Blaum, K. Icker, P. Mller, A. Schmitt, K. Wendt, and B. Wiche, Eur. Phys. J. D **2**, 33 (1998).
- [19] D.J.Berkeland and M.G.Boshier, Phys. Rev. A **65**, 033413 (2002).
- [20] S. Bize, S. Diddams, U. Tanaka, C. Tanner, W. Oskay, R. Drullinger, T. Parker, T. Heavner, S. Jefferts, L. Hollberg, et al., Phys. Rev. Lett. **90**, 150802 (2003).
- [21] G. Janik, W. Nagourney, and H. Dehmelt, J. Opt. Soc. Am. B **2**, 1251 (1985).
- [22] D. Berkeland, J. Miller, J. Bergquist, W. Itano, and D. Wineland, J. Appl. Phys. **83**, 5025 (1998).
- [23] W. Itano, I. Lewis, and D. Wineland, Phys. Rev. A **25**, 1233 (1982).
- [24] K. A. L. Database, *Cdrom 23*, <http://cfa-www.harvard.edu/amdata/ampdata/kurucz23/sekur.html> (2003).
- [25] W. Itano, J. Res. Natl. Inst. Stand. Technol. **105**, 829 (2000).
- [26] I. Sobelman, *Atomic spectra and radiative transitions* (Springer-Verlag, 1992).
- [27] B. Bransden and C. Joachain, *Physics of atoms and molecules* (Longman scientific and technical, 1994).
- [28] P. Gill, G. Barwood, G. Huang, H. Klein, P. Blythe, K. Hosaka, R. Thompson, S. Webster, S. Lea, and H. Margolis, *Trapped ion optical frequency standards*, EGAS 2003, Bruxelles, to be published in Physica Scripta (2003).
- [29] H. Häffner, S. Gulde, M. Riebe, G. Lancaster, C. Becher, J. Eschner, F. Schmidt-Kaler, and R. Blatt, Phys. Rev. Lett. **90**, 143602 (2003).
- [30] A. Bauch, Meas. Sci. Technol. **14**, 1159 (2003).